Multielectron excitations probed by helicity-modulation XMCD at *K*-edge in 3*d* transition metal compounds

Naomi Kawamura ,[a]* Tatsuya Yamamoto ,[b] Hiroshi Maruyama ,[b] Isao Harada ,[b] Motohiro Suzuki [c] and Tetsuya Ishikawa [ac]

[a]SPring-8/RIKEN, 1-1-1 Kouto, Mikaduki, Hyogo 679-5148, Japan, [b]Department of Physics, Facility of Science, Okayama University, 3-1-1 Tsushima-naka, Okayama 700-8530, Japan, [c]SPring-8/JASRI, 1-1-1 Kouto, Mikaduki, Hyogo 679-5198, Japan. E-mail: naochan@spring8.or.jp

Multielectron excitations (MEE) have been investigated using X-ray magnetic circular dichroism (XMCD) at the *K*-edge in 3*d* transition metal compounds. In the range of 50-70 eV above the absorption edge, a dichroic signal that is associated with MEE was identified. This phenomenon is thought to occur due to the super Coster-Kronig transition described as the final states $(1s)^1(3p)^5(3d)^{n+2}$ resulting from the 3*p* → 3*d* transitions. In order to verify this interpretation, XMCD measurements using the helicity-modulation method and calculations of the dichroic spectrum were performed based on this super Coster-Kronig transition.

Keywords: X-ray magnetic circular dichroism, multielectron excitations, super Koster-Kronig transition

1. Introduction

Photoexcitation is generally considered to be a single-electron excitation process, whereby the absorption of a photon leads to the ejection of an inner-core electron. However, a small probability exists that the removal of a core electron will cause excitation of additional electrons in the same atom. These phenomena including the shake-up and shake-off processes, and auto-ionization, have generally been neglected because they typically have small cross sections. Synchrotron radiation has a high-brilliance and well defined polarization and therefore has recently led to a better understanding of these phenomena opening up interesting subjects in this field.

Multielectron excitations (MEE) are classified as a secondary process in X-ray absorption. MEE in 3*d* transition metal (TM) compounds have been studied using X-ray absorption spectroscopy (XAS) and X-ray photoemission spectroscopy techniques (Bianconi *et al.*, 1991). However, the observed MEE effects in XAS are small and difficult to characterize experimentally or analyze quantitatively. X-ray magnetic circular dichroism (XMCD) is a powerful tool for studying electronic and magnetic states of absorbing atoms, and has been widely applied to various ferromagnetic materials. The XMCD spectrum is very sensitive to subtle changes in the electronic states due to the interplay between spin-orbit coupling and exchange interactions. An XMCD signal associated with an MEE process (XMCD-MEE) was first observed in the range of 110-150 eV at the $L_{2,3}$-edges in rare-earth (Dartyge *et al.*, 1992).

In the range of 50-70 eV above the *K*-edge of a 3*d* element, a dichroic signal has been observed in TM magnetic materials and identified as a phenomenon associated with MEE. We propose that this signal is due to the super Coster-Kronig mechanism described as the final states $(1s)^1(3p)^5(3d)^{n+2}$ resulting from the 3*p* → 3*d* transitions (Kawamura *et al.*, 1999). In order to verify this interpretation, we have performed XMCD measurement again using the helicity-modulation method (Suzuki *et al.*, 1998) and calculated the dichroic spectrum based on the mechanism.

2. Experimental

The following powdered samples were prepared in the present study: MFe$_2$O$_4$ (M=Mn, Fe, Co, Ni, and Cu), $Y_3Fe_5O_{12}$ (Y-IG), MnB, Fe_2B, Fe_3C, Fe_4N, Cu_2MnAl, and Co_2MnSi. All the samples are ferri- or ferromagnetic materials having a spontaneous magnetizaion at room temperature. In metallic compounds except for Heusler alloys, the magnetic moments of Mn or Fe are small in relation to the ligand-to-metal charge-transfer (Sugiura *et al.*, 1964) as compared with that of pure Fe or ferrites. These powdered samples were mounted uniformly on Scotch tapes for the X-ray absorption measurement.

The XMCD spectra were recorded in the transmission mode using the helicity-modulation (HM) method (Suzuki *et al.*, 1998) with a fixed magnetic field of 0.62 Tesla on the undulator beamline 39XU of SPring-8 (Goto *et al.*, 1998; Hayakawa *et al.*, 1998; Maruyama *et al.*, 1999). The beamline was composed of a rotated-inclined double-crystal monochromator (Yabashi *et al.*, 1999) equipped with a Si 111 crystal and a flat Pt-coated mirror for higher harmonics rejection. A diamond phase retarder was used in the Laue geometry with the 220 reflection plane in order to produce circularly polarized X-rays having plus and minus helicities in the a.c. mode with a frequency of 40 Hz by using a piezo oscillator. The X-ray intensity was monitored using an ionization chamber filled with N_2 gas before and after observing the sample. The degree of circular polarization was estimated to be 0.9 in the energy range used, as determined by polarization analysis. Energy resolution was estimated to be $\Delta\varepsilon / \varepsilon < 1.0 \times 10^{-4}$ at 7.110 keV. Absorption edge energy E_0 was taken at the first inflection point of XANES in metallic materials and at the pre-peak energy in the oxides. The energy position of XMCD-MEE E_1 was defined as the first peak position determined by some Lorentzian curves fit to the spectrum.

3. Results and Discussion

Figure 1 shows the XMCD spectra at the *M K*-edge in several 3*d* TM compounds as a function of the relative energy to the absorption edge. The XMCD shows a complicated profile around the edge, and the MEE process also yields a significant dichroic signal in the higher energy range, as indicated by the arrows in the figure. This dichroic signal is distinguishable from magnetic EXAFS oscillation because of large difference in wavelength, and evidently shows that magnetic effect is superimposed on the XAS spectrum. The focus of the present paper is on the XMCD-MEE signal observed in the energy range of 50 to 70 eV. The signal is of the same order as the XMCD spectrum having an intensity on the order of 10^{-3}. Although no significant structure is seen in the relevant energy region of the XAS spectrum, more fine structure is observed in the XMCD spectrum, because the S/N ratio is remarkably improved using the HM technique.

A positive structure is observed for all edges except for the Mn *K*-edge in $MnFe_2O_4$ and the Cu *K*-edge in $CuFe_2O_4$. $MnFe_2O_4$ exhibits a dispersion-type spectrum changing the sign from negative to positive with increasing photon energy. The first peak

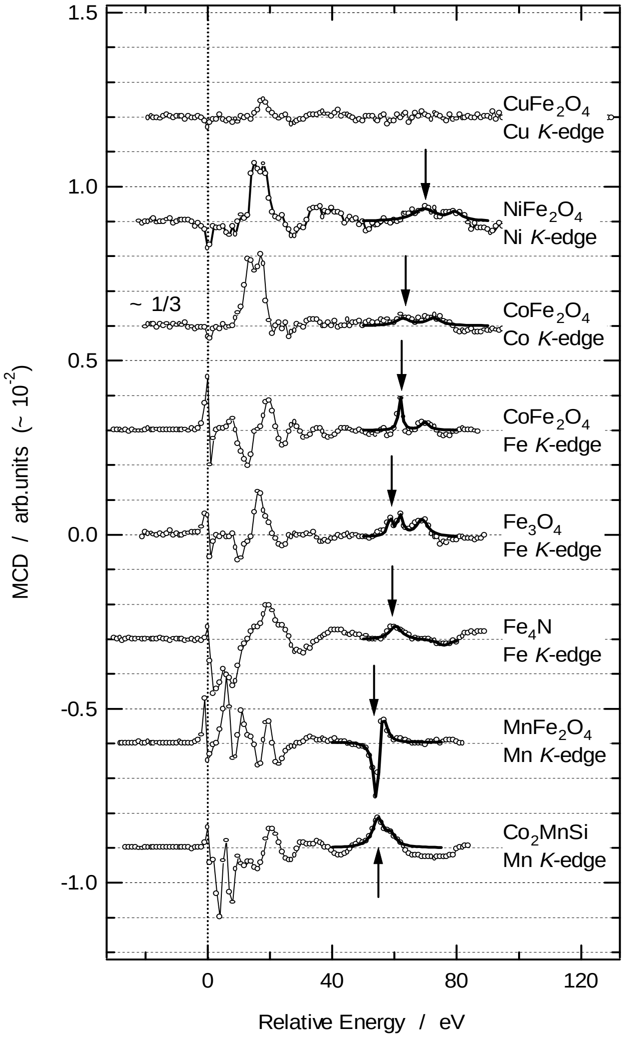

Figure 1
XMCD spectra at the *M K*-edge of several 3*d* TM compounds as a function of the relative energy from the absorption edge. The arrow indicates the position of XMCD-MEE. The solid line indicates the fitting result obtained using Lorentzian lineshapes.

of XMCD-MEE in MnFe$_2$O$_4$ shows a negative sign, which corresponds to the fact that the magnetic moments of Mn ions couple antiparallel to the Fe moments that are responsible for the major contribution. Therefore, the sign of XMCD-MEE appears to reflect the direction of the magnetic moments of the absorbing atom. Figure 1 indicates that the energy, E_1, of the XMCD-MEE increases with the atomic number (Z), although E_1 is almost constant irrespective of the materials at the same absorption edge (see in Fig. 2). Figure 2 shows that a linear relationship exists between the energy difference $\Delta E=(E_1-E_0)$ and Z holds over a wide range of the 3*d* elements. Moreover, ΔE is related to the $M_{2,3}$-edge energy of the (Z+1) atom, which corresponds to the 3*p* → 3*d* dipole transitions. This Z-dependence shows that the XMCD-MEE is closely related to 3*d* orbitals in TM because the dichroic signal reflects the magnetic states of the absorbing atom.

In the case of MFe$_2$O$_4$, the width of the profile is broadened and the intensity is decreased with increasing atomic number of the absorbing atom. Finally the XMCD-MEE signal disappears at the Cu *K*-edge. In metallic compounds, the XMCD-MEE signal exhibits a smaller intensity in comparison with that of insulators, which may be related to the decrease of the 3*d* hole number by the charge-transfer through the hybridization between the ligand *p*- and metal 3*d* orbitals. In order to clarify the relationship between the integrated intensity of XMCD-MEE and the atomic number, the integrated intensity is plotted as a function of Z in figure 3. The integrated intensity decreases with Z, corresponding to the decrease of the 3*d* hole number. Fe^{3+} and Mn^{2+} ions are expected to show a similar spectrum because of the same 3d^5 configuration. However, this is not the case. MFe$_2$O$_4$ (M=Fe~Cu), Fe ions in tetrahedral sites couple antiparallel to that in octahedral sites, so that the respective contributions of the antiparallel Fe ions tend to cancel each other. In metallic Mn and Fe compounds, the weak intensity is due to the charge-transfer effect from ligand atoms. This result indicates that the XMCD-MEE intensity is closely related to the 3*d* occupation of the absorbing atom. The disappearance of the XMCD-MEE signal at the Cu *K*-edge is consistent with the fact that MEE is impossible for the 3d^9 electronic configuration of Cu^{2+} ion, so that a super Coster-Kronig transition in which two electrons are excited to the 3*d* orbital as suggested by Kawamura *et al.* (1999) is supported.

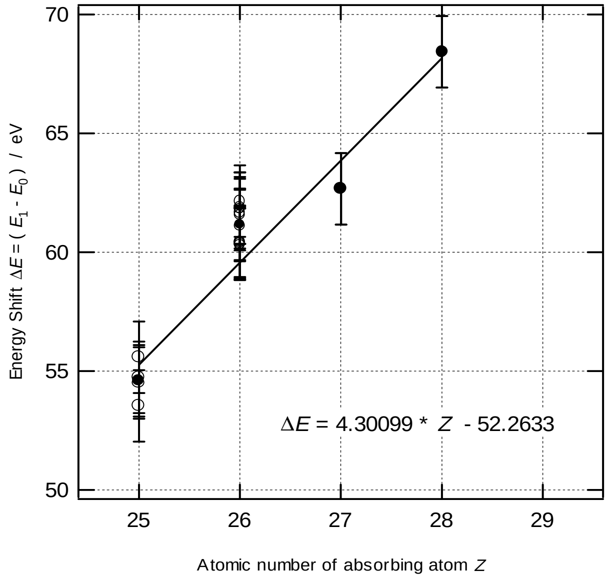

Figure 2
The energy difference $\Delta E=(E_1-E_0)$ is plotted as a function of Z of the absorbing atom for the various magnetic materials. The solid line shows the fitting results for the linear function. White circles indicate the peak energy E_1 in the metallic compounds (MnB, Cu$_2$MnAl, Co$_2$MnSi, Fe$_2$B, Fe$_3$C and Fe$_4$N). Closed circles indicate E_1 in ferrites MFe$_2$O$_4$ (M=Mn, Fe, Co, Ni and Cu).

We have proposed that the MEE phenomenon is due to a super Coster-Kronig transition described by the final state $(1s)^1(3p)^5(3d)^{n+2}$ resulting from the 3*p* → 3*d* transitions. In order to confirm this assumption, we calculated the XMCD-MEE spectrum based on this mechanism for the Fe^{3+} ion. In this simple calculation, many-body-effects originating in the crystal structure are ignored. As a result, the energy position is in good agreement with the experimental observations. The integrated intensity is related to the occupation of 3*d* electrons. However, a dispersion-type profile contradicts these observations. This result implies that the mechanism of XMCD-MEE is associated with the super Coster-Kronig transition. The existence of the ligand atoms and the orbital moment in the initial states must be taken into consideration in order to reproduce the spectral profiles.

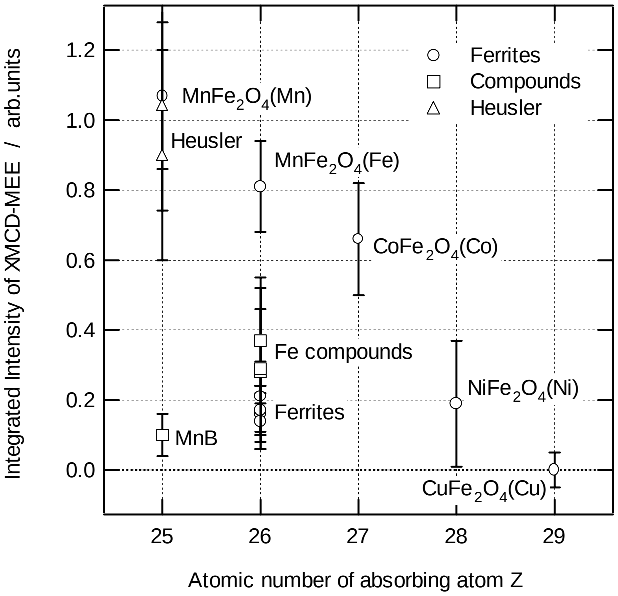

Figure 3
The integrated intensity of XMCD-MEE as a function of *Z*. The intensity is the integrated first peak obtained by a Lorentzian curve fit to the XMCD-MEE spectrum.

4. Conclusion

We measured XMCD spectra at the *K*-edge in a series of 3*d* transition metal compounds and observed a characteristic dichroic signal associated with the MEE phenomenon in the range 50 to 70 eV above the edges. The presence of super Coster-Kronig transitions is strongly suggested by the sign of the profile, the energy position, the dependence of the integrated intensity on the atomic number of the absorbing atoms, as well as theoretical calculations using a simple model. The XMCD-MEE phenomena are expected to become a useful tool for investigating 3*d* electronic states.

The authors are deeply indebted to Professor K. Okada for taking part in several useful discussions. We would like to thank to Dr. A. Baron for his help in preparing the manuscript. This work was performed with the approval of the Japan Synchrotron Radiation Research Institute (JASRI) (Proposal No. 1997B0155-NS-np) and under the Special Postdoctoral Researchers Program of RIKEN.

References

Bianconi, A., Garcia, J., Benfatto, M., Marcelli, A., Natoli, C. R., & Ruiz-Lopez, M. F. (1991). *Phys. Rev.* **B43**, 6885-6892.

Dartyge E., Fontaine, A., Guirgetti, Ch., Pizzini, S., Baudelet, F., Krill, G., Brouder, Ch., & Kappler, J.-P. (1992) *Phys. Rev.* **B61**, 3155-3158.

Goto, S., Yabashi, M., Ohashi, H., Kimura, H., Takeshita, K., Uruga, T., Mochizuki, T., Kohmura, Y., Kuroda, M., Yamamoto, M., Furukawa, Y., Kamiya, N., & Ishikawa, T. (1998). *J. Synchrotron Rad.* **5**, 1202-1205.

Hayakawa, S., Goto, S., Shoji, T., Yamada, E., & Gohshi, Y. (1998). *J. Synchrotron Rad.* **5**, 1114-1116.

Kawamura, N., Maruyama, H., Kobayashi, K., Uemura, S., Urata, A., & Yamazaki, H. (1999). *J. Phys. Soc. Jpn.* **68**, 923-929.

Maruyama, H., Suzuki, M., Kawamura, N., Ito, M., Arakawa, E., Kokubun, J., Hirano, K., Horie, K., Uemura, S., Hagiwara, K., Mizumaki, M., Goto, S., Kitamura, H., Namikawa, K., & Ishikawa, T. (1999). *J. Synchrotron Rad.* **6**, 1133-1137.

Sugiura, T., Itoh, F., Takaki, H., Nakamura, Y., & Shikazono, N. (1964). *J. Phys. Soc. Jpn.* **19**, 1252.

Suzuki, M., Kawamura, N., Mizumaki, M., Urata, A., Maruyama, H., Goto, S., & Ishikawa, T. (1998). *Jpn. J. Appl. Phys.* **37**, L1488-L1490.

Yabashi, M., Yamazaki, H., Tamasaku, K., Goto, S., Takeshita, K., Mochizuki, T., Yoneda, Y., Furukawa, Y., & Ishikawa, T. (1999). *SPIE Conf. Proc.*, **3773**, 2-13.

Received 31 July 2000 • Accepted 10 November 2000